Asian Journal of Chemistry; Vol. 35, No. 12 (2023), 2939-2947

ASIAN JOURNAL OF CHEMISTRY

https://doi.org/10.14233/ajchem.2023.30254

Adsorption of Antibiotic Drug on the Surface of Humic Acid Modified Magnetite Nanoparticles: Kinetics, Isotherm and Thermodynamic Studies

ARTI JANGRA, RAMESH KUMAR*, JAI KUMAR and JAIVEER SINGH

Department of Chemistry, Kurukshetra University, Kurukshetra-136119, India

*Corresponding author: E-mail: rameshkumarkuk@gmail.com; rameshchemkuk@kuk.ac.in

Received: 4 September 2023; *Accepted*: 5 October 2023; *Published online*: 2 December 2023; AJC-21453

The present study reports the synthesis of humic acid-modified magnetite nanoparticles for adsorption behaviour towards the ofloxacin drug. Several analytical and spectroscopic techniques were used to characterize the synthesized surface modified magnetite nanoparticles. In order to determine the highest possible adsorption capacity of these coated nanoparticles, the effects of various influencing variables such as pH of the solution, contact time, initial concentration of adsorbate solution, amount of adsorbent and temperature were also investigated using batch adsorption method. Adsorption isotherm and kinetic analysis for the adsorption of ofloxacin drug from aqueous solution were studied simultaneously. The kinetics and isotherm studies demonstrated good agreement with the pseudo-second-order kinetics model and Langmuir model of isotherm, respectively. Thermodynamic analysis of the adsorption of ofloxacin on the surface of humic acid modified magnetite nanoparticles displayed negative values of Gibb's free energy change, positive values of enthalpy as well as entropy change, resulting that the adsorption process was spontaneous and endothermic in nature. A comparative study of percentage drug removal efficiency of humic acid functionalized magnetite nanoparticles with the reported adsorbents has also been reported. This study revealed that the humic acid-modified magnetite nanoparticles showed remarkable adsorption capacity and thus could be used as an effective adsorbent for the removal of ofloxacin from aqueous solution.

Keywords: Adsorption, Humic acid, Magnetite nanoparticles, Ofloxacin.

INTRODUCTION

Pharmaceuticals are regarded as the most prominent class of organic contaminants which have adverse effects on environment [1]. Contaminations by drugs mainly antibiotics, have hostile effects on living organism [2,3]. Antibiotics, a category of pharmaceuticals, have been emphasized due to their widespread application in human and other animals. Ofloxacin (OFL) is a fluorinated quinolone of the second generation and a pyridine carboxylic acid derivative [4,5]. It is an antibiotic that is used to prevent and cure several bacterial diseases. It is a novel class of quinolone composed of several different compounds. These are also found in ground and surface water and thus can be easily enter into aquatic animals and human. Thus, their presence in the environment is considered as a threat to human and aquatic lives [6,7]. Therefore, it is essential to eliminate these harmful pharmaceutical contaminants from the environment so that their unnecessary entry can be prevented into the bodies of human and other animals.

For this purpose, adsorption [8], chemical oxidation [9] and photo-catalytic reduction [10] are the appropriate strategies that are used frequently in the process of removing ofloxacin drug pollutant from wastewater. Out of which, the adsorption method is the one that has received the most attention because of its comparatively low cost, flexibility and higher selectivity. Several researchers used different kinds of adsorbent materials for the adsorption of drug pollutant from aqueous solution such as Hao *et al.* [11] used polymerized ionic liquid@3-trimethoxysilyl propyl methacrylate@Fe_3O_4 nanoparticles for adsorption of sulphonamide and quinolone from water sample [11]. Li *et al.* [12] used kaolinite for the exclusion of ciprofloxacin from aqueous solution. Kundu *et al.* [13] synthesized Ni-doped Ti-O_2 nanoparticles and employed these as adsorbent for the adsorption of ofloxacin from aqueous solution. Peñafiel *et al.* [14] used organic residues for the adsorption of ciprofloxacin drug pollutant from aqueous solution. In recent years, the synthesis and surface functionalization of magnetic nanoparticles have received a great deal of interest due to their remarkable charac-

teristics like biocompatibility, superparamagnetic properties and high surface-to-volume ratio [15,16] that makes them wonderful adsorbents. Parashar *et al.* [17] used magnetic iron oxide nanoparticles for the removal of oxcarbazepine from aqueous solution. Several coating materials were being used to modify the surface of magnetite nanoparticles. Jangra *et al.* [18] used citric acid as the coating material to modify the surface of magnetite nanoparticles and further employed as adsorbent for the removal of ciprofloxacin drug from aqueous solution . Recently, humic acid coated magnetite nanoparticles as an adsorbent for the adsorption of crystal violet dye and imidacloprid pesticide from aqueous solution has been reported [19,20]. In response to the findings of abovesaid studies, we have extended our studies for the removal of ofloxacin drug from aqueous solutions using humic acid coated magnetite nanoparticles. The present study also exhibited the influences of several experimental variables such as pH of the solution, contact time, amount of adsorbent, initial concentration of adsorbate solution and temperature on the percentage ofloxacin removal efficiency of synthesized nano-adsorbent with the help of batch adsorption method. Moreover, the isotherm, kinetics as well as thermodynamic studies were also investigated.

EXPERIMENTAL

Chemicals of analytical grade including ferrous sulfate heptahydrate ($Fe_2SO_4·7H_2O$), ferric chloride hexahydrate ($FeCl_3·6H_2O$), humic acid (HA) and ammonium hydroxide (25%) were purchased from SRL (India). Distilled water was used to prepare the solutions. Ofloxacin (OFL) drug was used as adsorbate throughout the experiments.

Characterization: Neat Fe_3O_4 and humic acid coated magnetite nanoparticles (HA@Fe_3O_4) were prepared with the help of a digital mechanical stirrer at 2000 rpm. The infrared spectra of pure humic acid, bare magnetite and humic acid modified magnetite nanoparticles were recorded using MB-3000 ABB FTIR spectrophotometer. Surface morphology and the average size of synthesized nanoparticles were measured by Hitachi SU-8000 filed emission scanning electron microscope (FESEM). Distilled water was used as dispersive solvent. The X-ray diffraction patterns of both neat Fe_3O_4 and humic acid modified magnetite nanoparticles were recorded using an instrument consisting vertical theta-theta goniometer having 2θ range of 20-80º working with Cu*K*α radiation of 1.540 Å wavelength at room temperature. A Perkin-Elmer STA-6000 thermogravimetric analyzer with 5-80 ºC/min heating rate and 20-1000 ºC temperature range was employed to obtain thermograms of the synthesized bare as well as humic acid modified magnetite nanoparticles. A T90 PG Instrument Limited UV-visible spectrophotometer in 900-190 nm range was used to record the UV spectra and absorbance of solutions of different concentrations.

Synthesis of neat Fe_3O_4 and humic acid modified magnetite nanoparticles: A simple and cost-effective method *i.e.* co-precipitation technique was used to synthesize neat Fe_3O_4 and humic acid modified magnetite nanoparticles [19,20]. Briefly, 4.2 g of $FeSO_4·7H_2O$ and 6.1 g of $FeCl_3·6H_2O$ were dissolved in 100 mL distilled water. The prepared mixture was heated upto 90 ºC and stirred continuously at 2000 rpm using a digital mechanical stirrer under N_2 atmosphere. After 20-30 min, a rapid addition of 10-15 mL NH_4OH solution (25 %) to the above mixture and further stirred for another 10-15 min (pH 9-10) resulted in the black coloured solution that confirmed the preparation of bare magnetite nanoparticles (Fe_3O_4). In order to modify the surface of bare magnetite nanoparticles, solution of humic acid was successfully added to the former prepared black colour solution with continuous stirring for about 30 min under same reaction conditions. Black coloured precipitates of humic acid modified magnetite nanoparticles were separated from the solution using an external magnetic field. Thus formed bare as well humic acid magnetite nanoparticles were washed with distilled water and dried using vacuum oven.

Ofloxacin drug adsorption study using humic acid modified magnetite nanoparticles: The synthesized humic acid modified magnetite nanoparticles were treated as nano-adsorbent for the effective adsorption of ofloxacin (OFL) drug from aqueous solution. Batch adsorption method was used to perform the adsorption experiments [21,22]. Effect of various experimental parameters including pH of the solution (2.0-8.0), contact time (0-120 min), temperature (298-313 K), amount of nano-adsorbent (5-30 mg) and initial concentration of adsorbate (OFL) solution (10-50 mg/L) on the adsorption of OFL drug was investigated. UV-visible spectrophotometer was used to measure the absorbance of OFL solutions before and after the completion of adsorption process at maximum wavelength *i.e.* 290 nm.

The adsorption capacity (q_e) and the percentage removal efficiency (% R) at equilibrium can be calculated using the following eqns. 1 and 2:

Adsorption capacity:

$$q_e = \frac{C_o - C_e}{m} \times V \quad (1)$$

Percentage removal efficiency:

$$R\ (\%) = \frac{C_o - C_e}{C_o} \times 100 \quad (2)$$

In present work, the isotherm models and kinetic models including Langmuir [23,24], Freundlich [25,26], Tempkin [27,28] isotherm models and pseudo-first-order [29,30] as well as pseudo-second-order [31,32] kinetic models were applied to investigate the behaviour and the rate mechanism of adsorption process.

RESULTS AND DISCUSSION

Characterization of synthesized bare and humic acid modified magnetite nanoparticles

FTIR spectral studies: The infrared spectral studies confirmed the coating over the surface of bare magnetite nanoparticles. IR spectra of neat Fe_3O_4 and humic acid modified magnetite nanoparticles were recorded and compared successfully. The IR spectra of bare magnetite nanoparticles depicted an intense peak near 600 cm^{-1} that can be attributed to Fe-O stretching vibration and the adsorption band around 3300 cm^{-1} may be associated with –OH stretching vibrations. Moreover, some new peaks at about 1638 cm^{-1} and 1416 cm^{-1} were appeared

in the IR spectrum of humic acid modified magnetite nanoparticles corresponding to asymmetric as well as symmetric stretching of carboxylate anion of humic acid, respectively [19]. The IR spectrum of modified magnetite nanoparticles displayed all peaks present in the IR spectrum of bare magnetite nanoparticles as well as pure humic acid. Thus, the overall results confirmed the successful coating of humic acid onto the surface of bare magnetite nanoparticles (Fig. 1).

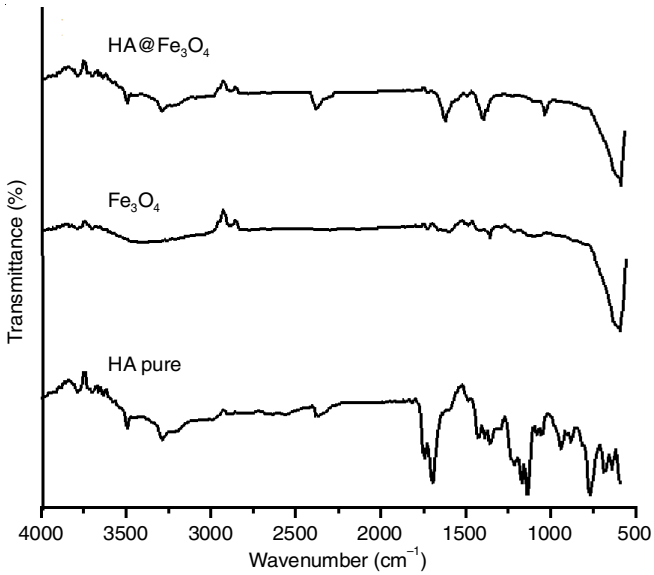

Fig. 1. FTIR spectra of bare Fe_3O_4 and HA@Fe_3O_4 nanoparticles

Morphological studies: The FESEM study was used to examine the average size as well as the surface morphology of the synthesized magnetite nanoparticles. The FESEM images confirmed that the average diameter of bare as well as humic acid modified magnetite nanoparticles was about 20 nm and 30 nm, respectively [20]. This enhancement in the size of nanoparticles revealed the effective coating of humic acid onto the surface of bare magnetite nanoparticles (Fig. 2).

X-ray diffraction studies: The X-ray diffractometer was used to record X-ray diffraction (XRD) patterns in 2θ range of 20-80º. The recorded XRD patterns of bare and the humic acid modified magnetite nanoparticles displayed several peaks (Fig. 3) which suggested about their semi-crystalline nature [19].

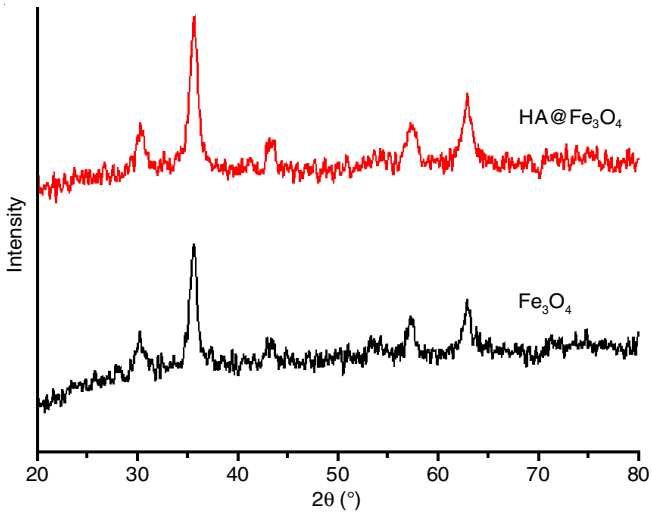

Fig. 3. XRD of bare Fe_3O_4 & HA@Fe_3O_4 nanoparticles

Thermogravimetric (TGA) studies: Thermogravimetric study was employed to confirm the successful coating over the surface of bare magnetite nanoparticles by comparing the thermograms of neat Fe_3O_4 and humic acid modified magnetite nanoparticles. Thermogravimetric curves of both bare and humic acid modified magnetite nanoparticles displayed weight

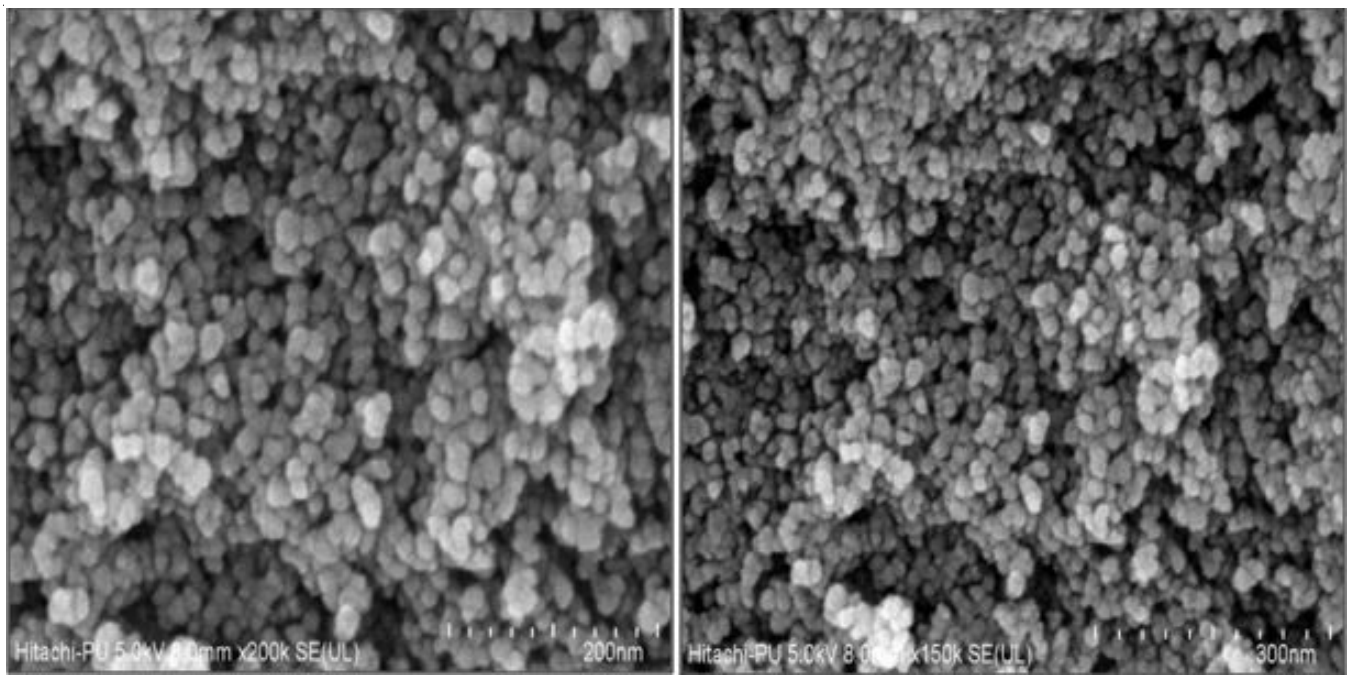

Fig. 2. FESEM image of bare Fe_3O_4 nanoparticles [1 division = 20 nm] and HA@Fe_3O_4 nanoparticles [1 division = 30 nm]

loss upto 100 ºC, which may be attributed to the loss of loosely bound water molecules (Fig. 4). In addition to this, no change in weight loss was observed for bare magnetite nanoparticles whereas a significant weight loss from 200 to 500 ºC was perceived that may be due to the thermal decomposition of humic acid [20].

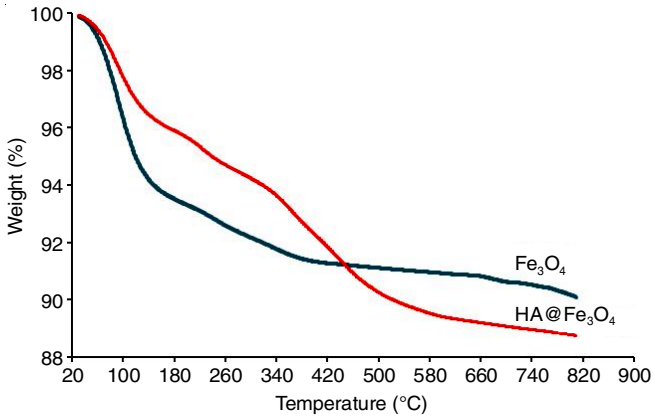

Fig. 4. TGA curves of bare Fe_3O_4 & HA@Fe_3O_4 nanoparticles

Batch adsorption analysis of HA@Fe_3O_4 nanoparticles: Several preliminary sorption experiments were executed to examine the influences of adsorption parameters on the adsorption capacity and percentage removal efficiency of HA@Fe_3O_4 nanoparticles.

Effect of pH of solution on the percentage removal efficiency of HA@Fe_3O_4 nanoparticles: The variation in pH of solution plays a significant role in adsorption as variation in pH affects the surface charge of both adsorbent and adsorbate (Fig. 5a). The effect of pH of solution can be investigated in pH range 2.0-8.0 using fixed amount of nanoadsorbent (20 mg) and at variable concentration of adsorbate solution. The percentage removal efficiency of synthesized humic acid modified magnetite nanoparticles for OFL drug increases steadily with the increase in pH of the solution from 2.0 to 8.0 (Fig. 5b). This increased effect might be associated with the occurrence of electrostatic interactions between adsorbate and adsorbent. At low pH, the surface of both synthesized nanoadsorbent and adsorbate *i.e.* OFL drug exhibited positive charge resulting electrostatic repulsions between them. A substantial decrease in the percentage OFL removal efficiency of synthesized nano-adsorbent (HA@Fe_3O_4) was observed due to these repulsions in acidic medium. On contrary, as the pH of solution increases the degree of protonation of surface decreases gradually suggesting improved the interactions among adsorbate and nano-adsorbent. As a result of these improved interactions, it may be stated that the percentage OFL drug removal efficiency increases with the increase in value of pH. Moreover, the maximum percentage removal efficiency was obtained at pH 8.0 that may be due to the zwitter-ionic or neutral behaviour of the adsorbate *i.e.* OFL [33] and the negatively charged surface of nano-adsorbent (HA@Fe_3O_4).

Effect of time on the percentage removal efficiency of HA@Fe_3O_4 nanoparticles and kinetic study: The effect of time plays a vital role in the determination of percentage removal efficiency of nano-adsorbent and kinetic study helped in the determination of rate mechanism of adsorption process. Batch adsorption method was used to investigate the effect of time (0-120 min) on the percentage removal efficiency of HA@Fe_3O_4 nanoparticles using fixed concentration of OFL drug solution (50 mg/L) and pH *i.e.* 8 for variable amount of adsorbent (HA@Fe_3O_4) at 1500 rpm stirring rate. The results depicted that the percentage OFL removal efficiency of nano-adsorbent displayed slow increase initially and after that a rapid increase was observed until the equilibrium stage attained (Fig. 6a). This behaviour suggested the presence of a large number of active adsorption sites on the surface of the nano-adsorbents, which are responsible for the effective adsorption of OFL drug from aqueous solution. However, as time progressed, the number of empty active sites was less available and filling of these sites became more challenging due to the increasing repulsive forces (between the adsorbate and the adsorbent). As a consequence,

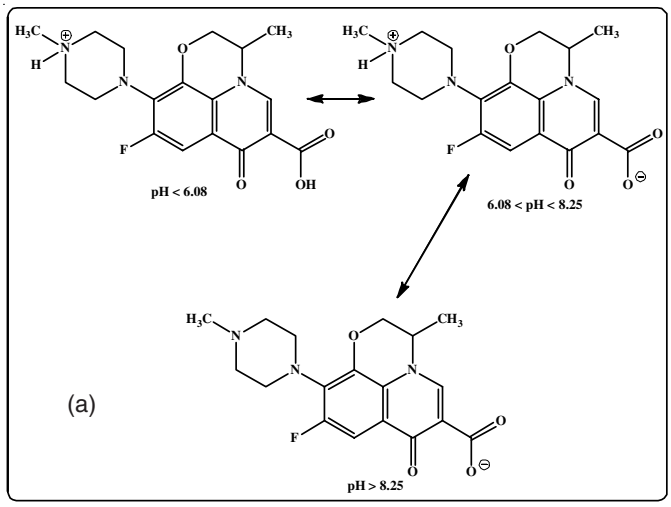

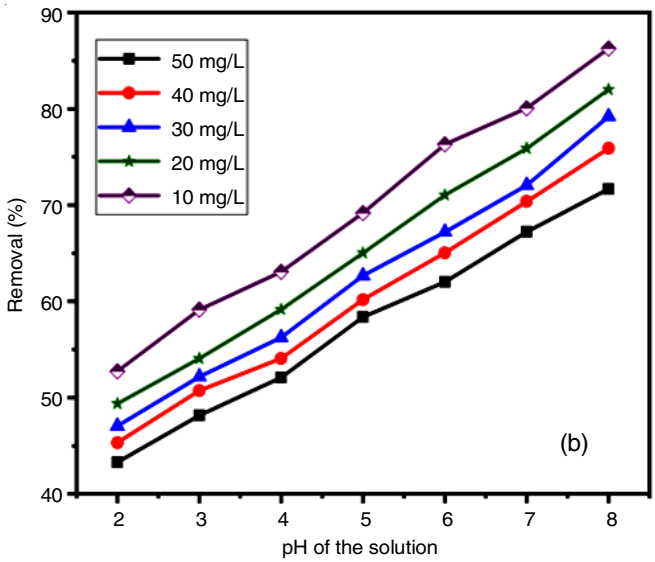

Fig. 5. Distribution of ofloxacin at different pH values (a) and Effect of pH on percentage removal efficiency of humic acid modified magnetite nanoparticles (b)

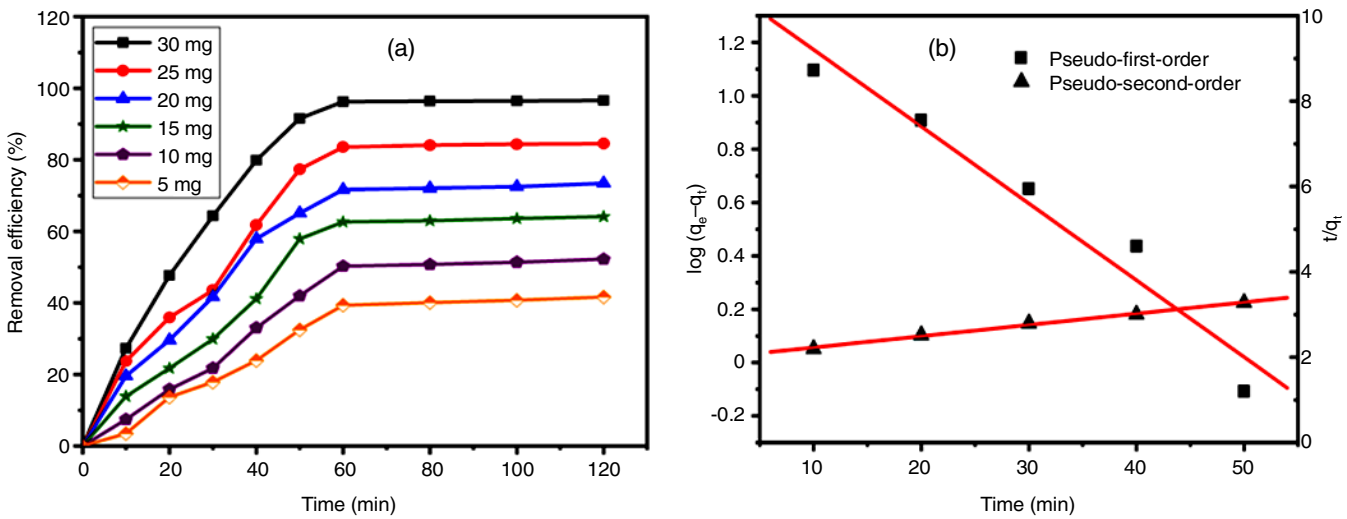

Fig. 6. Effect of contact time on percentage removal efficiency of humic acid modified magnetite nanoparticles (a) and kinetic orders (b)

the percentage removal efficiency of synthetic nano-adsorbent steadily increased. Moreover, based upon these studies, several kinetic models including pseudo-first-order (eqn. 3) and pseudo-second-order (eqn. 4) kinetic models were applied to examine the rate mechanism of adsorption process.

$$\log(q_e - q_t) = \log q_e - \frac{k_1 t}{2.303} \quad (3)$$

$$\frac{t}{q_t} = \frac{1}{k_2 q_e^2} + \frac{t}{q_e} \quad (4)$$

where q_e (mg/g) and q_t (mg/g) represents the adsorption capacity at equilibrium and at any time t; k_1 and k_2 denotes the rate constants for pseudo-first-order and pseudo-second-order kinetic models, respectively. The values of these parameters can be calculated by plotting graphs for their respective kinetic models and are summarized in Table-1. By comparing the values of correlation coefficients (R^2) of these models, it may be suggested that the adsorption kinetics was found to obey the pseudo-second-order of kinetics resulting the existence of chemisorption phenomenon for the adsorption of OFL pollutants on the surface of nano-adsorbent (Fig. 6b).

TABLE-1
PARAMETERS OF KINETIC ORDERS

Kinetic order	Correlation coefficient (R^2)	Rate constant
Pseudo-first-order	0.9355	0.066 min^{-1}
Pseudo-second-order	0.9931	0.00035 g/mg min

*R^2 denotes the correlation coefficients.

Effect of amount of adsorbent on percentage removal efficiency of HA@Fe_3O_4 nanoparticles: The impact of amount of synthesized nano-adsorbent on percentage OFL removal efficiency from aqueous solution was investigated using fixed volume (10 mL) of adsorbate (OFL) solution of different concentrations (10-50 mg/L), fixed pH *i.e.* 8 and variable amount of adsorbent (5-30 mg) with stirring rate of 1200-1500 rpm. The findings of these investigations revealed that the percentage OFL removal efficiency of nano-adsorbent (HA@Fe_3O_4) increased upon increasing the amount of synthesized nano-adsorbent (Fig. 7). These results can be justified by the fact that the increased amount of nano-adsorbent provides more active sites for adsorption and large surface area for the adsorption process [34]. A maximum of 96.28 % of OFL drug was successfully adsorbed from the aqueous solution for 30 mg of nano-adsorbent.

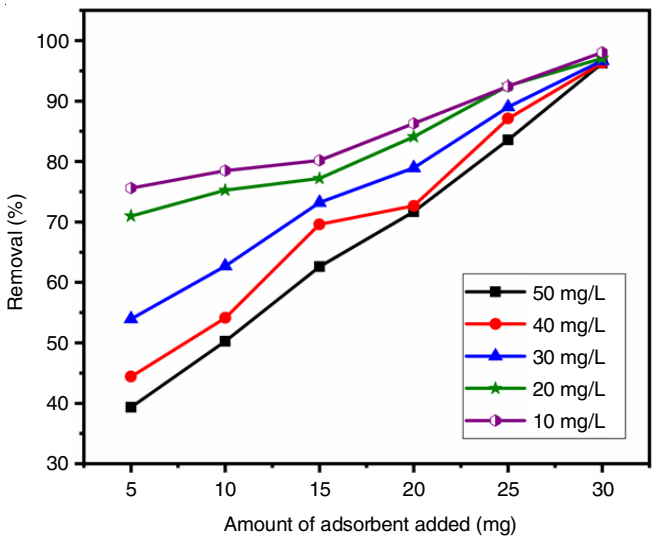

Fig. 7. Effect of amount on percentage removal efficiency of humic acid modified magnetite nanoparticles

Effect of initial concentration of adsorbate solution on percentage removal efficiency: The influence of initial concentration of adsorbate (OFL drug) solution on the percentage removal efficiency of synthesized nano-adsorbents was investigated using adsorbate solutions of variable concentrations (10-50 mg/L) for different amounts of nano-adsorbent (5-30 mg) under optimum conditions such as equilibrium time, temperature and pH. The findings indicated that as the concentration of adsorbate *i.e.* OFL solutions increased, the percentage removal efficiency decreased because a particular quantity of adsorbent provides a fixed number of active sites (Fig. 8a).

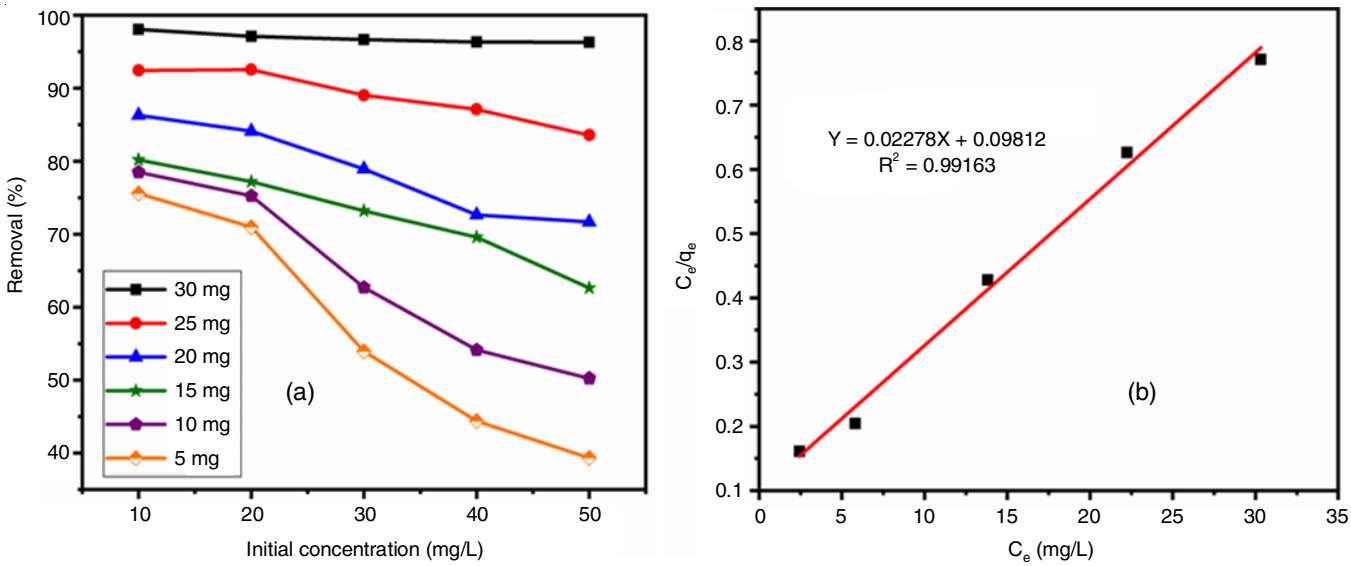

Fig. 8. Effect of initial concentration of ofloxacin drug solution on percentgae removal efficiency of humic acid modified magnetite nanoparticles (a) and Langmuir isotherm model (b)

Adsorption isotherm study: Based upon the above mentioned investigations, the isotherm models such as Langmuir, Freundlich as well as Temkin isotherm models were applied to examine the nature of interactions involved in between adsorbate and adsorbent during adsorption process. Langmuir model of isotherm suggests a single layer adsorption *i.e.* the adsorption of adsorbate occurs on homogenous surface whereas Freundlich model of isotherm describes a multilayer adsorption that occurs on the surface of adsorbate heterogeneously. Moreover, Tempkin model of isotherm predicts that the heat of adsorption of all adsorbent molecule decreases in a linear manner which may be due to the covering of adsorbent surface. The adsorption capacity of the synthesized nano-adsorbent for the OFL adsorption can be measured using fixed concentration of adsorbent *i.e.* 0.5 g/L. Linearized form (eqns. 5-7) of above mentioned isotherm models were applied simultaneously to examine the applicability of these models of isotherm.

$$\frac{C_e}{q_e} - \frac{1}{bq_m} + \frac{C_e}{q_m} \quad (5)$$

$$\log q_e = \log K_F + \frac{1}{n}\log C_e \quad (6)$$

$$q_e = B\ln A + B\ln C_e, \quad B = \frac{RT}{b} \quad (7)$$

where C_e (mg/L) and q_e (mg/g) are the concentration of solution and adsorption capacity of adsorbent at equilibrium point; q_m (mg/g) denotes the maximum adsorption capacity and T (K) is the temperature; K_F, b and A represents the Freundlich, Langmuir and Temkin constants, respectively.

These equations were used to plot graphs, which further helped in the calculations of different experimental isotherm parameters (Fig. 8b). The value of correlation coefficient (R^2) of Langmuir isotherm was found to be greater (0.99163) than that of others, which inferred that the adsorption process was found to fit better with Langmuir model of isotherm with 43.89 mg/g maximum adsorption capacity for the adsorption of OFL drug from aqueous solution (Table-2).

Effect of temperature on percentage removal efficiency of HA@Fe_3O_4 and thermodynamic study: Temperature is generally considered as one of the most significant parameter that have an impact on the nature and favourability of adsorption process [35]. Several experiments were performed to examine the effect of temperature on (298-313 K) on the OFL percentage removal efficiency of synthesized nano-adsorbent (HA@Fe_3O_4) using fixed amount of nano-adsorbent (30 mg) and fixed volume (10 mL) of OFL solution of 50 mg/L concentration at optimum pH *i.e.* 8.0. The results of the study suggested that the percentage OFL removal efficiency of nano-adsorbent increased with the increase in temperature until 313 K. Thus, 313 K could be considered as the optimum temperature for the maximum adsorption (Fig. 9a).

Based upon these studies, the values of several thermodynamic variables including gibbs free energy change (ΔG), enthalpy change (ΔH) and entropy change (ΔS) were calculated

TABLE-2
VALUES OF ISOTHERM PARAMETERS

Langmuir			Freundlich			Temkin		
R^2	q_m (mg/g)	b (L/mg)	R^2	n	K_F (mg/g)	R^2	A (L/mg)	B (J/mol)
0.9916	43.89	0.232	0.8560	2.890	3.013	0.9295	0.00266	0.107

*R^2 denotes the correlation coefficients, q_m is the maximum adsorption capacity, b is the Langmuir constant, n and K_F are the Freundlich constants, A and B are the Temkin constants.

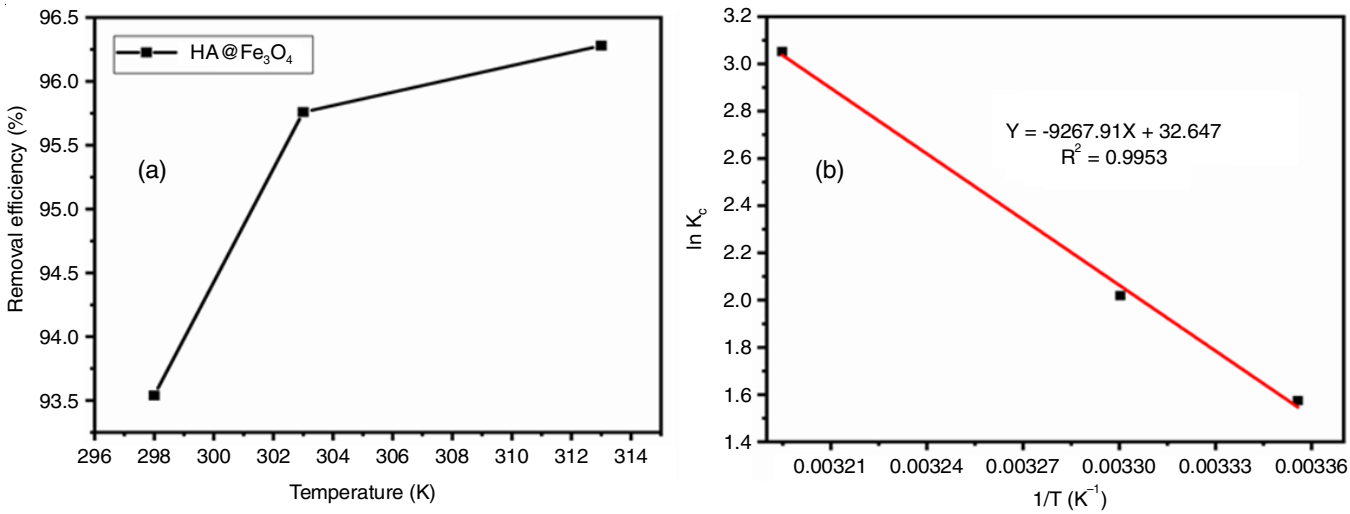

Fig. 9. Effect of temperature on percentage removal efficiency of humic acid modified magnetite nanoparticles (a) and thermodynamic study (b)

using following equations (eqns. 8-11) to explain the spontaneity feasibility and favourability of adsorption process.

$$\Delta G = \Delta H - T\Delta S \quad (8)$$

$$\Delta G = -RT \ln K_c \quad (9)$$

$$K_c = \frac{q_e}{C_e} \quad (10)$$

$$\ln K_c = \frac{\Delta S}{R} - \frac{\Delta H}{RT} \quad (11)$$

where T is temperature (K); R is universal gas constant (8.314 J mol^{-1} K); q_e is adsorption capacity (mg/g) and C_e is the concentration (mg/L) at equilibrium point.

The above equations were used to plot the graph between log K_c and 1/T. The values of intercept and slope of the plotted graph helped in the calculation of of ΔS and ΔH values (Fig. 9b). Thus, obtained negative values of ΔG (Gibb's free energy change) depicted about the spontaneity and favourability of adsorption process while the positive values of entropy as well as enthalpy change specified about the high degree of freedom as well as endothermic behaviour of the adsorption process, respectively (Table-3).

TABLE-3
VALUES OF THERMODYNAMIC PARAMETERS

Temp. (K)	ln K_c	ΔG (kJ/mol)	ΔH (kJ/mol K)	ΔS (J/mol K)
298	1.574	-3.900	77.053	271.42
303	2.018	-5.085		
313	3.051	-7.941		

*K_c denotes the equilibrium constant. ΔG, ΔH and ΔS denote the change in gibbs free energy, enthalpy and entropy, respectively.

Comparative studies: The percentage drug removal efficiency of humic acid functionalized magnetite nanoparticles has been compared with drug removal efficiency shown by various reported adsorbents including multi-walled carbon nanotubes [36], titanium dioxide nanoparticles [37], citric acid modified magnetite nanoparticles [18], rice husk ash [38], agricultural waste [39], rGO-molybdenum disulfide [40], UV-activated persulfate [41], Ni-doped titanium dioxide [13] and *Moringa oleifera* pod husks [42] (Table-4). In addition, humic acid was also used as effective adsorbent for the removal of several other antibiotics including fluoroquinolone [43], ciprofloxacin [44,45], oxytetracycline [46], tetracycline [47], *etc.* (Table-5). From this comparative study, it is clear that humic acid functionalized magnetite nanoparticles have been found as most potential candidate as compared to above mentioned adsorbents for the removal of drug residues from the aqueous solution.

TABLE-4
PERCENTAGE REMOVAL EFFICIENCY OF SEVERAL ADSORBENTS FOR DRUG POLLUTANTS

Adsorbents	Removal (%)
Citric acid modified magnetite nanoparticles	87.58
Titanium dioxide nanoparticles	94.00
Multi-walled carbon nanotubes	94.50
Rice husk ash	85.00
Agricultural waste	85.00
rGO-Molybdenum disulfide	95.00
UV-activated persulfate	94.35
Ni-doped titanium dioxide nanoparticles	70.00
Moringa oleifera pod husks	90.98
Humic acid	96.28

TABLE-5
LIST OF SEVERAL DRUG POLLUTANTS ADSORBED BY HUMIC ACID (ADSORBENT)

Adsorbents	Adsorbate
Coating magnetic biochar with humic acid	Fluoroquinlone
Humic acid modified magnetite nanoparticles	Ciprofloxacin
Humic acid modified hydrogel beads	Ciprofloxacin
Lanthanum modified magnetic humic acid	Oxytetracycline
Iron functionalized carbonized humic acid	Tetracycline

Conclusion

Present work emphasized on the application of humic acid functionalized magnetite nanoparticles for the adsorption of

ofloxacin drug from the aqueous solution *via* batch adsorption method in which humic acid coated magnetite nanoparticles were prepared. The effect of several experimental factors such as pH of the solution, contact time, temperature, initial concentration of the adsorbate solution and amount of nano-adsorbent on the percentage ofloxacin removal efficiency of nano-adsorbent was investigated. The findings of these investigations revealed that the adsorption process achieved equilibrium point after 60 min at specific pH *i.e.* 8.0 with 96.28 % removal of ofloxacin for 30 mg of nano-adsorbent. Furthermore, the kinetic study suggested that the adsorption process was found to follow pseudo-second-order of kinetics suggesting the chemisorption phenomenon. The isotherm parameters depicted that the adsorption process was found to obey Langmuir isotherm model with 49.89 mg/g maximum adsorption capacity. While thermodynamic study explained the spontaneous and endothermic nature of adsorption of ofloxacin drug on the surface of humic acid modified magnetite nanoparticles. Moreover, the comparative study of percentage drug removal efficiency of humic acid functionalized magnetite nanoparticles with other adsorbents reached to the conclusion that the surface coated magnetite nanoparticles reported in the present paper have remarkable drug adsorption efficiency among all adsorbents. Therefore, the overall study concluded that the synthesized humic acid modified magnetite nanoparticles can be treated as effective and efficient nano-adsorbent for the adsorption of ofloxacin drug from the aqueous solution.

ACKNOWLEDGEMENTS

Two of the co-authors, Arti Jangra and Jai Kumar are highly thankful to Kurukshetra University, Kurukshetra, India for providing research facilities. The authors are grateful to UGC, New Delhi, India, for providing the financial support in the form of Senior Research Fellowship.

CONFLICT OF INTEREST

The authors declare that there is no conflict of interests regarding the publication of this article.

REFERENCES

1. D. Fatta-Kassinos, S. Meric and A. Nikolaou, *Anal. Bioanal. Chem.*, **399**, 251 (2011); https://doi.org/10.1007/s00216-010-4300-9
2. M. Bilal, S. Mehmood, T. Rasheed and H.M.N. Iqbal, *Curr. Opin. Environ. Sci. Health*, **13**, 68 (2020); https://doi.org/10.1016/j.coesh.2019.11.005
3. T. Mackulak, S. Cernanský, M. Fehér, L. Birošová and M. Gál, *Curr. Opin. Environ. Sci. Health*, **9**, 40 (2019); https://doi.org/10.1016/j.coesh.2019.04.002
4. B. Ebrahimpour, Y. Yamini and M. Moradi, *J. Pharm. Biomed. Anal.*, **66**, 264 (2012); https://doi.org/10.1016/j.jpba.2012.03.028
5. H. Titouhi and J.E. Belgaied, *J. Environ. Sci.*, **45**, 84 (2016); https://doi.org/10.1016/j.jes.2015.12.017
6. M. Mezzelani, S. Gorbi and F. Regoli, *Mar. Environ. Res.*, **140**, 41 (2018); https://doi.org/10.1016/j.marenvres.2018.05.001
7. X. Zhang, J. Li, S. Yan, R.D. Tyagi and J. Chen, Physical, Chemical, and Biological Impact (Hazard) of Hospital Wastewater on Environment: Presence of Pharmaceuticals, Pathogens and Antibiotic-resistance Genes; In: Current Developments in Biotechnology and Bioengineering, Elsevier, pp. 79–102 (2020); https://doi.org/10.1016/B978-0-12-819722-6.00003-1
8. A. Khadir, A. Mollahosseini, R.M.A. Tehrani and M. Negarestani, A Review on Pharmaceutical Removal from Aquatic Media by Adsorption: Understanding the Influential Parameters and Novel Adsorbents, In: Sustainable Green Chemical Processes and their Allied Applications. Nanotechnology in the Life Sciences, eds.: A. Inamuddin, Springer, Cham., *Nanotechnol. Life Sci.*, 207 (2020); https://doi.org/10.1007/978-3-030-42284-4_8
9. H. Farzaneh, K. Loganathan, J. Saththasivam and G. McKay, *Sci. Total Environ.*, **765**, 142704 (2021); https://doi.org/10.1016/j.scitotenv.2020.142704
10. A. Javaid, S. Latif, M. Imran, N. Hussain, M.S.R. Rajoka, H.M.N. Iqbal and M. Bilal, *Chemosphere*, **291**, 133056 (2022); https://doi.org/10.1016/j.chemosphere.2021.133056
11. H. Wu, Y. Shi, X. Guo, S. Zhao, J. Du, H. Jia, L. He and L. Du, *J. Sep. Sci.*, **39**, 4398 (2016); https://doi.org/10.1002/jssc.201600631
12. Z. Li, H. Hong, L. Liao, C.J. Ackley, L.A. Schulz, R.A. MacDonald, A.L. Mihelich and S.M. Emard, *Colloids Surf. B Biointerfaces*, **88**, 339 (2011); https://doi.org/10.1016/j.colsurfb.2011.07.011
13. P. Kundu, A. Kaur, S.K. Mehta and S.K. Kansal, *J. Nanosci. Nanotechnol.*, **14**, 6991 (2014); https://doi.org/10.1166/jnn.2014.9238
14. M.E. Peñafiel, J.M. Matesanz, E. Vanegas, D. Bermejo, R. Mosteo and M.P. Ormad, *Sci. Total Environ.*, **750**, 141498 (2021); https://doi.org/10.1016/j.scitotenv.2020.141498
15. S.H. Huang and R.S. Juang, *J. Nanopart. Res.*, **13**, 4411 (2011); https://doi.org/10.1007/s11051-011-0551-4
16. N. Elahi and M. Rizwan, *Artif. Organs*, **45**, 1272 (2021); https://doi.org/10.1111/aor.14027
17. A. Parashar, S. Sikarwar and R. Jain, *Int. J. Environ. Anal. Chem.*, **102**, 117 (2022); https://doi.org/10.1080/03067319.2020.1716977
18. A. Jangra, J. Singh, J. Kumar, K. Rani and R. Kumar, *Indian J. Biochem. Biophys.*, **59**, 892 (2022); https://doi.org/10.56042/ijbb.v59i9.59916
19. A. Jangra, J. Singh, R. Khanna, P. Kumar, S. Kumar and R. Kumar, *Asian J. Chem.*, **33**, 3031 (2021); https://doi.org/10.14233/ajchem.2021.23471
20. A. Jangra, J. Kumar, D. Singh, H. Kumar, P. Kumar, S. Kumar and R. Kumar, *Water Sci. Technol.*, **86**, 3028 (2022); https://doi.org/10.2166/wst.2022.379
21. A. Jangra, S. Kumar, J. Singh, J. Kumar, K. Rani, P. Kumar, D. Singh and R. Kumar, *Biointerface Res. Appl. Chem.*, **13**, 1 (2023); https://doi.org/10.33263/BRIAC135.480
22. N. Ghosh, S. Sen, G. Biswas, A. Saxena and P.K. Haldar, *Water Air Soil Pollut.*, **234**, 202 (2023); https://doi.org/10.1007/s11270-023-06217-8
23. F. Golmohammadi, M. Hazrati and M. Safari, *Microchem. J.*, **144**, 64 (2019); https://doi.org/10.1016/j.microc.2018.08.057
24. I. Langmuir, *J. Am. Chem. Soc.*, **40**, 1361 (1918); https://doi.org/10.1021/ja02242a004
25. X. Weng, W. Cai, G. Owens and Z. Chen, *J. Clean. Prod.*, **319**, 128734 (2021); https://doi.org/10.1016/j.jclepro.2021.128734
26. H. Freundlich, *Z. Phys. Chem.*, **57U**, 385 (1907); https://doi.org/10.1515/zpch-1907-5723
27. A.V. Samrot, H.H. Ali, J. Selvarani A, E. Faradjeva, R. P, P. P and S. Kumar S, *Curr. Res. Green Sustain. Chem.*, **4**, 100066 (2021); https://doi.org/10.1016/j.crgsc.2021.100066
28. V. Temkin and M.J. Pyzhev, *Acta Physicochim. URSS*, **12**, 217 (1940).
29. K.L. Tan and B.H. Hameed, *J. Taiwan Inst. Chem. Eng.*, **74**, 25 (2017); https://doi.org/10.1016/j.jtice.2017.01.024
30. S. Lagergren, *Kungliga Svenska Vetenskap. Handlingar*, **24**, 1 (1898).

31. Y.S. Ho and G. McKay, *Process Biochem.*, **34**, 451 (1999); https://doi.org/10.1016/S0032-9592(98)00112-5
32. Z. Jeirani, C.H. Niu and J. Soltan, *Rev. Chem. Eng.*, **33**, 491 (2017); https://doi.org/10.1515/revce-2016-0027
33. L.E. Vîjan, *Optoelectron. Adv. Mater. Rapid Commun.*, **3**, 60 (2009).
34. J. Singh, A. Jangra, K. Rani, P. Kumar, S. Kumar and R. Kumar, *Asian J. Chem.*, **33**, 2675 (2021); https://doi.org/10.14233/ajchem.2021.23377
35. A.H. Birniwa, A.S. Abubakar, H.N.M.E. Mahmud, S.R.M. Kutty, A.H. Jagaba, S.S. Abdullahi and Z.U. Zango, Application of Agricultural Wastes for Cationic Dyes Removal from Wastewater, In: Textile Wastewater Treatment. Sustainable Textiles: Production, Processing, Manufacturing & Chemistry, S.S. Muthu and A. Khadir, Eds. Springer: Singapore, pp. 239-274 (2022); https://doi.org/10.1007/978-981-19-2832-1_9
36. M.C. Ncibi and M. Sillanpää, *J. Hazard. Mater.*, **298**, 102 (2015); https://doi.org/10.1016/j.jhazmat.2015.05.025
37. A.M. Aljeboree and A.F. Alkaim, *J. Phys. Conf. Ser.*, **1294**, 052059 (2019); https://doi.org/10.1088/1742-6596/1294/5/052059
38. A. Thakur, N. Sharma and A. Mann, *Mater. Today Proc.*, **28**, 1514 (2020); https://doi.org/10.1016/j.matpr.2020.04.833
39. S.A. Hassan and F.J. Ali, *Int. J. Adv. Sci. Technol. Res.*, **2**, 950 (2014).
40. A. Jaswal, M. Kaur, S. Singh, S.K. Kansal, A. Umar, C.S. Garoufalis and S. Baskoutas, *J. Hazard. Mater.*, **417**, 125982 (2021); https://doi.org/10.1016/j.jhazmat.2021.125982
41. P. Tavassoli, E. Bazrafshan, F.K. Mostafapour, Z. Maghsoodi, D. Balarak, H. Kamani and A.A. Zarei, *J. Mazandaran Univ. Med. Sci.*, **27**, 116 (2018) (In Persian).
42. R.A. Wuana, R. Sha'Ato and S. Iorhen, *Adv. Environ. Res.*, **4**, 49 (2015); https://doi.org/10.12989/aer.2015.4.1.049
43. J. Zhao, G. Liang, X. Zhang, X. Cai, R. Li, X. Xie and Z. Wang, *Sci. Total Environ.*, **688**, 1205 (2019); https://doi.org/10.1016/j.scitotenv.2019.06.287
44. S.T. Danalioglu, S.S. Bayazit, Ö. Kerkez, B.G. Alhogbi and M. Abdel Salam, *Chem. Eng. Res. Des.*, **123**, 259 (2017); https://doi.org/10.1016/j.cherd.2017.05.018
45. M.Z. Afzal, R. Yue, X.F. Sun, C. Song and S.G. Wang, *J. Colloid Interface Sci.*, **543**, 76 (2019); https://doi.org/10.1016/j.jcis.2019.01.083
46. C. Yan, L. Fan, Y. Chen and Y. Xiong, *Colloids Surf. A Physicochem. Eng. Asp.*, **602**, 125135 (2020); https://doi.org/10.1016/j.colsurfa.2020.125135
47. D. Xie, H. Zhang, M. Jiang, H. Huang, H. Zhang, Y. Liao and S. Zhao, *Chin. J. Chem. Eng.*, **28**, 2689 (2020); https://doi.org/10.1016/j.cjche.2020.06.039